

The mechanism of bursting oscillations with different codimensional bifurcations and nonlinear structures

Qinsheng Bi · Shaolong Li · Juergen Kurths · Zhengdi Zhang

Received: 12 January 2015 / Accepted: 13 March 2016 / Published online: 6 April 2016
© Springer Science+Business Media Dordrecht 2016

Abstract The main purpose of this article is to demonstrate that bursting oscillations can be observed not only in the slow–fast autonomous dynamical systems with multiple scales associated with time domain, but also in the non-autonomous dynamical systems with periodic excitations when an order gap exists between the exciting frequency and the natural frequency, implying multiple scales in frequency domain. Furthermore, we try to investigate the influence of different codimensional bifurcations between the quiescent states (QS) and repetitive spiking states (SP) and the nonlinear structures with different equilibrium branches on the bursting oscillations. By introducing an inductor as well as a periodically changed electrical current source in a traditional Chua’s circuit and taking suitable parameter values, a modified four-dimensional periodically excited oscillator with multiple scales in frequency domain is established. Bursting oscillations for two cases with nonlinear terms up to third and fifth order with codimension-1 and codimension-

2 bifurcations have been explored, respectively. It is found that more equilibrium states may exist when higher order nonlinear terms are introduced in the vector field, which may cause multiple quiescent states, and accordingly, multiple forms of repetitive spiking oscillations in one bursting attractor, leading to more complicated bursting phenomena. Furthermore, instead of jumping from one stable equilibrium branch to settle down to another stable equilibrium branch when codimension-1 bifurcations (fold bifurcations) exist between QSs and SPs, codimension-2 bifurcation (fold-Hopf bifurcation) may cause QS approximately located on one stable equilibrium branch to jump to repetitive spiking oscillations surrounding another stable equilibrium branch of the generalized autonomous system.

Keywords Periodic excitation · Multiple time scales · Bursting oscillation · Bifurcation mechanism

The authors are supported by the National Natural Science Foundation of China (21276115, 11272135, 11472115, 11472116) and Qinlan Project of Jiangsu.

Q. Bi (✉) · S. Li · Z. Zhang
Faculty of Science, Jiangsu University, Zhenjiang 212013,
People’s Republic of China
e-mail: qbi@ujs.edu.cn

J. Kurths
Potsdam Institute for Climate Impact Research,
Telegrafenberg A31, 14473 Potsdam, Germany
e-mail: Juergen.Kurths@pik-potsdam.de

1 Introduction

Many dynamical systems in natural and engineering problems involve two time scales [1,2], which often behave in periodic states characterized by a combination of relatively large-amplitude and nearly harmonic small-amplitude oscillations, conventionally denoted by N^K with N and K corresponding to large and small amplitude oscillations, respectively [3,4]. Generally, we say the system is in quiescent state (QS) stage when

all the variables are at rest or exhibit small-amplitude oscillations [5]. The coupling of two time scales may lead the systems to spiking state (SP), in which the variables may behave in large-amplitude oscillations [6,7]d. Bursting phenomena can be observed when the variables alternate between QS and SP. Two important bifurcations associated with the bursters exist: bifurcation of a quiescent state to repetitive spiking and bifurcation of a spiking attractor to quiescence [8,9].

At the beginning of the analysis for the dynamical systems with multiple time scales, a obvious method is introduced by eliminating the slow variables upon solving the related equations [10]. Perturbation method is also employed to find the asymptotic solutions by expanding all the variables in terms of small parameters [11]. Many other approaches have been developed to investigate the dynamics, which, however, cannot be used to explore the interaction between different time scales, until the so-called slow–fast analysis method is introduced [12–14]. By dividing the whole system into two subsystems, i.e., the fast subsystem and the slow subsystem [15], Qs and SPs as well as the bifurcations between them may be approximated by the equilibrium states as well as the related bifurcation forms in the fast subsystem, while the slow system can be used to understand the slow passage effect on the moderation of QS and SP [16,17].

Based on the slow–fast analysis, a lot of results related to dynamics with two time scales are presented, in which several bursting oscillations such as the fold/fold [18] and fold/Hopf [19] bursters are obtained. However, most of the reports are focused on the autonomous systems, in which obvious slow and fast subsystems can be obtained [20], while for non-autonomous systems, such as periodically excited systems, when an order gap exists between the frequency of periodic excitation and natural frequency, no obvious slow and fast subsystem exists, while the effect of two time scales can also be observed [21], on the fact that the trajectories of systems are related to both the two frequencies [22], behaving in relaxation oscillations [23]. Here we define the frequency of the free vibration of autonomous nonlinear dynamical system as the natural frequency of the related nonlinear system. Unlike the linear system, the natural frequency of the nonlinear system is related to the dynamical behaviors, which may change with the parameters of the system. For example, when the trajectory settles down to a focus, the natural frequency can be deter-

mined by the imaginary parts of the pair of the conjugate eigenvalues of the focus, while when the system behaves in periodic movement, the natural frequency can be described by the frequency of the oscillation. Since no obvious slow and fast subsystem exists, the method of slow–fast analysis [24] can not be directly employed to approach the mechanism of the bursting. How to explore the characteristics of the multi-mode oscillations in non-autonomous system still remains an open problem. For the typical periodically excited dynamical system, when the exciting term changes on a much smaller time scale comparing with the original system, the whole exciting term can be regarded as a slow-varying parameter, leading to the so-called generalized autonomous and the transformed phase portrait can be employed to explore the influence of the exciting term on the evolution of the dynamical behavior [25].

Furthermore, up to now, only codimension-1 bifurcations [26,27], such as fold bifurcation and Hopf bifurcations, exist between QS and SP and only one form of QS and SP [28,29] involves in the most of bursting oscillations reported [30,31]. How the bursting oscillations behave when higher codimensional bifurcations or multiple forms of Qs and SPs involve in the dynamics still need to be explored.

Here we introduce an inductor as well as a periodically changed electrical power in a traditional Chua's circuit [32] and taking suitable parameter values so that not only an order gap exists between the excited frequency and the natural frequency, but also different codimensional bifurcations as well as multiple equilibrium branches may involve in generalized autonomous system corresponding to the oscillations, the evolution of the dynamics of the system is investigated and different types of bursting oscillations as well as the bifurcation mechanism will be presented.

2 Mathematical model

Based on the canonical three-dimensional Chua's model [32], a modified version has been constructed with a controller composed of an inductor as well as a linear resistor, which may exhibit more complex dynamics [33]. By introducing a periodically changed electrical current source in the model with a nonlinear resistor, shown in Fig. 1, the related mathematical model can be expressed as

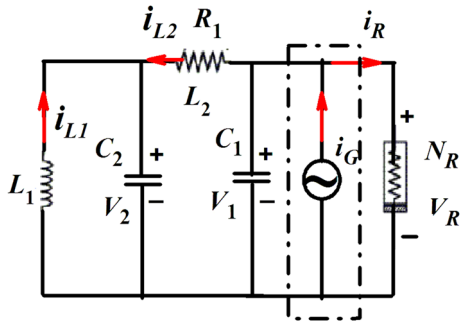


Fig. 1 Circuit with periodic excitation

$$\begin{aligned}
 \frac{dV_1}{dt} &= \frac{1}{C_1} [G_1(V_2 - V_1) - G_1 g(V_1) + I_G \sin(\omega t)], \\
 \frac{dV_2}{dt} &= \frac{1}{C_2} [G_1(V_1 - V_2) + i_{L1} + i_{L2}], \\
 \frac{di_{L1}}{dt} &= -\frac{1}{L_1} (V_2 - R_2 i_{L2}), \\
 \frac{di_{L2}}{dt} &= -\frac{1}{L_2} V_2,
 \end{aligned}
 \tag{1}$$

where $G_1 = 1/R_1$, $G_2 = 1/R_2$, while $g(V_1) = \Delta_1 V_1 + \Delta_2 V_1^3 + \Delta_3 V_1^5$ describes the relationship between the current and the voltage passing across the nonlinear resistor, in which Δ_1 is a non-dimensional parameter, while Δ_2 and Δ_3 corresponds to the dimension $(v)^{-2}$ and $(v)^{-4}$, respectively.

By introducing the transformations $V_1 = E_{10} x$, $V_2 = E_{20} y$, $i_{L1} = \frac{E_{20}}{R_1} u$, $i_{L2} = \frac{E_{20}}{R_1} v$, $t = R_1 C_2 \tau$ and taking $R_2 = \frac{L_1}{R_1 C_2}$, (1) can be written in the non-dimensional form as

$$\begin{aligned}
 \frac{dx}{d\tau} &= \alpha [y - \delta f(x)] + w, \\
 \frac{dy}{d\tau} &= \kappa x - y + u + v, \\
 \frac{du}{d\tau} &= -\gamma y + v, \\
 \frac{dv}{d\tau} &= -\beta y,
 \end{aligned}
 \tag{2}$$

where E_{10} and E_{20} is used as the references and $\alpha = \frac{C_2 E_{20}}{R_1 E_{10}}$, $\beta = \frac{R_1^2 C_2}{L_2}$, $\kappa = \frac{E_{20}}{E_{10}}$, $\delta = \frac{E_{20}}{E_{10}} (1 + \Delta_1)$, $\gamma = \frac{R_1^2 C_2}{L_1}$, $f(x) = ax + bx^3 + cx^5$ with $a = 1.0$, $b = \frac{\Delta_3 E_{10}^2}{1 + \Delta_1}$, $c = \frac{\Delta_5 E_{10}^4}{1 + \Delta_1}$, $w = A \sin(\Omega \tau)$ with $A = \frac{I_G R_1 C_2}{C_1 E_{10}}$, $\Omega = \omega R_1 C_2$. System (2) with no external excitation may evolve from stable fixed point to periodic orbit and to chaos. Furthermore, super-chaotic movement can be observed for certain parameter values, corresponding to two positive Lyapunov exponents [34]. The external excitation may also cause the oscillator to evolve from periodic orbit to chaotic movements. However, when an order gap exists between Ω and the natural frequency of the autonomous oscilla-

tor, the effect of two time scales may appear. Here we fix the parameter $\Omega = 0.005$ and other parameters at $O(1.0)$. Obviously, the state variables x, y, u, v may oscillate mainly according to the natural frequency, i.e., $O(dx/d\tau, dy/d\tau, du/d\tau, dv/d\tau) \approx O(1.0) \equiv T_1$, while the exciting term w oscillates periodically according to another much smaller scale, i.e., $O(dw/d\tau) \approx O(0.005) \equiv T_2$, leading to the coupling between two scales T_1 and T_2 , which may cause the bursting oscillations in the system.

3 Bifurcation analysis of the generalized autonomous system

Since the state variables may oscillate mainly according to the natural frequency, for $\Omega \ll \Omega_N$, where Ω_N represents the natural frequency, during an arbitrary period T_N , ($T_N = 2\pi/\Omega_N$) i.e., $\tau \in [\tau_0, \tau_0 + T_N]$, the exciting term w may change between $w_A = A \cos(\Omega \tau_0)$ and $w_B = A \cos[\Omega(\tau_0 + \tau_N)]$, implying $w_A \approx w_B$, which means w keeps almost a constant during any arbitrary period T_N . Therefore, (2) can be considered as a generalized autonomous system, in which w may be regarded as a slow-varying parameter though w may vary between $-A$ and $+A$. It can also be understood from the fact that the autonomous system (2) forms the fast subsystem, while $w = A \cos(\Omega \tau)$ forms the slow subsystem.

Now we turn to the bifurcation analysis of the generalized autonomous system on regarding the periodic external excitation as a parameter w . The equilibrium point of (2) can be expressed in the form $E Q(x, y, u, v) = (X_0, 0, -\kappa X_0, 0)$, where X_0 satisfies

$$\alpha \delta (X_0 + bX_0^3 + cX_0^5) + w = 0,
 \tag{3}$$

the stability of which can be determined by the associated characteristic equation, written in the form

$$\lambda^4 + h_1 \lambda^3 + h_2 \lambda^2 + h_3 \lambda + h_4 = 0,
 \tag{4}$$

where

$$\begin{aligned}
 h_1 &= 1 + \alpha \delta (1 + 3bX_0^2 + 5cX_0^4), \\
 h_2 &= \beta + \gamma - \alpha \kappa + \alpha \delta (1 + 3bX_0^2 + 5cX_0^4), \\
 h_3 &= \beta + \alpha \delta (1 + 3bX_0^2 + 5cX_0^4), \\
 h_4 &= \alpha \beta \delta (1 + 3bX_0^2 + 5cX_0^4).
 \end{aligned}
 \tag{5}$$

Obviously, E_Q is stable for $h_1 > 0, h_4 > 0, h_1h_2 - h_3 > 0$ and $h_1h_2h_3 - h_1^2h_4 - h_3^2 > 0$, resulting in two possible bifurcation sets. One can be expressed in the form $h_4=0$, i.e.,

$$\begin{cases} 1 + 3bX_0^2 + 5cX_0^4 = 0, \\ 1 + bX_0^3 + cX_0^5 = 0, \end{cases} \tag{6}$$

on which fold bifurcation may occur, causing jumping phenomenon between different equilibrium points, while the other can be written in the form

$$\begin{aligned} h_1h_2h_3 - h_1^2h_4 - h_3^2 &= 0, \\ (h_1 > 0, h_4 > 0, h_1h_2 - h_3 > 0), \end{aligned} \tag{7}$$

on which Hopf bifurcation may take place, leading to periodic oscillation with the frequency $\Omega_H = \frac{h_3}{h_1}$.

Furthermore, a codimension-2 bifurcation with a zero and a pair of pure imaginary eigenvalues $\pm\sqrt{\beta}I$ as well as negative eigenvalue -1 takes place on the set

$$\begin{cases} a + 3bX_0^2 + 5cX_0^4 = 0, \\ a + bX_0^3 + cX_0^5 = 0, \\ \alpha\kappa - \gamma = 0, \end{cases} \tag{8}$$

leading to the occurrence of limit cycle away from the original fixed point.

As an example, the bifurcation sets on the plane (κ, w) for the parameters fixed at $\alpha = 8.0, \beta = 0.5, \gamma = 8.0, \delta = -0.15, b = -2.0, c = 0.0$ are presented in Fig. 2a, which divide the parameter plane into eight regions corresponding to different dynamical behaviors. In Region (1) and (8), only one stable equilibrium point exists corresponding to EB_1 and EB_3 in Fig. 2b, respectively. On the fold bifurcation set F_1 , two equilibrium branch EB_2 and EB_3 meet each other, which leads to a cusp point, together with a stable equilibrium point related to EB_1 . While on the fold bifurcation set F_2 , EB_1 and EB_2 meet each other, leading to a cusp point, together with a stable equilibrium point related to EB_3 . On the Hopf bifurcation sets H_1 , the stable focus related to EB_1 loses its stability to form a limit cycle, while on H_2 , the stable focus related to EB_3 bifurcates to another limited cycle.

In region (2) and (5), a stable focus related to EB_1 as well as a stale limit cycle bifurcated from the equilibrium branch EB_3 can be observed, while in Region (4) and (6), a stable focus related to EB_3 as well as a

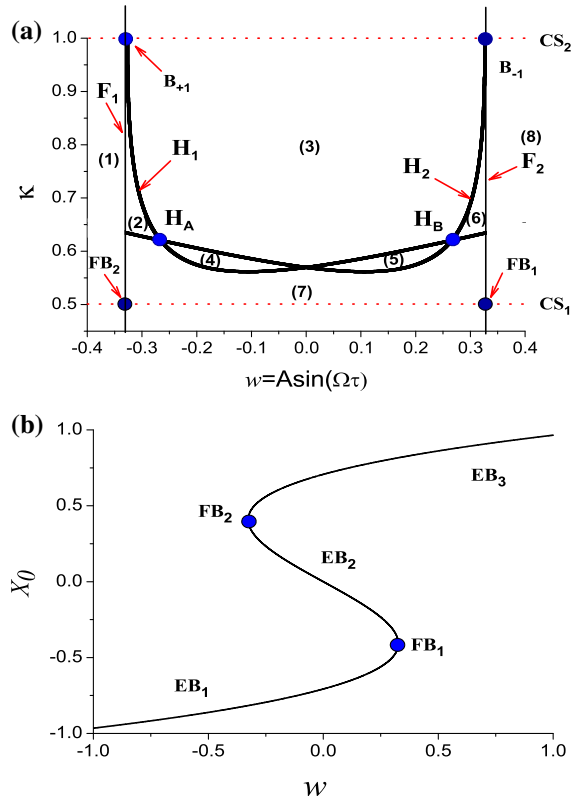


Fig. 2 Bifurcations for $\alpha = 8.0, \beta = 0.5, \gamma = 8.0, \delta = -0.15, b = -2.0, c = 0$. **a** Bifurcation sets on the (κ, w) plane **b** equilibrium branches with the variation of w

stale limit cycle bifurcated from the equilibrium branch EB_1 exists. Two stable cycles bifurcate from equilibrium branches EB_1 and EB_3 , respectively, in Region (3). However, in Region (7), two stable foci related to EB_1 and EB_3 as well as a saddle point can be obtained.

At the two intersection points B_{+1} and B_{-1} of the bifurcation sets F_1 and H_1 or F_2 and H_2 , codimension two bifurcations of the equilibrium points corresponding to a zero as well as a pair of pure imaginary eigenvalues take place, which leads to different behaviors in the neighboring regions of B_{+1} and B_{-1} , respectively, with small parameter perturbation.

However, at the intersection points H_A and H_B of H_1 or H_2 , instead of a codimension two bifurcation, two codimension one bifurcations (super-Hopf bifurcations) corresponding to the equilibrium points located on EB_1 and EB_3 , respectively, take place, leading to different limit cycles.

Remark 1 \odot There also exist other forms of bifurcations for certain values of parameters, which we omitted here for simplicity, since these bifurcation conditions are so special that they may not really exist for the real systems. Furthermore, for certain fixed parameters, not all the above bifurcation sets can be observed, since the original stable fixed point may lose the stability via only one bifurcation form.

\odot The bifurcation sets can be obtained by continuation method, using a properly continuation package for continuous-time system, such as MATCONT [35], which is a standard tool for numerical bifurcation analysis. Here we only list the conditions for the bifurcations, which may be used for the investigation of the bursting oscillations caused by the interaction between different time scales.

4 Evolution of bursting oscillations as well as the mechanism

Because of the order gap between the exciting frequency and the natural frequency, bursting oscillations, which always behave in the combination of small- and large-amplitude oscillations, can be observed. Note that the form of nonlinear function $f(x)$ may influence the attractors of bursting oscillations. When higher-order nonlinear terms are introduced in the function, more equilibrium points of the generalized autonomous system can be observed, which may lead to more complicated bursting oscillations. Furthermore, the forms of the bifurcations between the quiescent states (QSs) and repetitive spiking states (SPs) may also affect the structures of bursting attractors. Here we fix the parameters at

$$\alpha = 8, \quad \beta = 0.5, \quad \gamma = 8, \quad \Omega = 0.005, \quad (9)$$

and consider the influence of the two factors, i.e., the nonlinear functions and the bifurcations between QSs and SPs, on the bursting oscillations.

We first introduce the conception of transformed phase portrait (TPP), in which the relationship between the variations of state variables and that of excited term will be presented, so that the bifurcation analysis above with the change of w can be employed to account for the mechanism of the bursting oscillations.

4.1 Transformed phase portrait (TPP)

Note that all the bifurcation analysis is investigated upon taking w as the bifurcation parameter, which may be employed to explore the mechanism of the bursting oscillations. Therefore, the relationship between the state variables and w is very important for the effect of two time scales on the dynamics, which can be described by the transformed phase portraits. The trajectory as well as w can be described as

$$\begin{aligned} \Pi_G &= [X(t), w] \\ &= \{[x(t), y(t), z(t), A \sin(\Omega t)], \forall t \in R\}, \end{aligned} \quad (10)$$

from which one may obtain the traditional phase portraits $\{[x(t), y(t), z(t)], \forall t \in R\}$, as well as its projections on subspaces such as $\{[x(t), y(t)], \forall t \in R\}$. Here we regard w as a generalized state variable and define Π_G changing with four variables (x, y, z, w) as well as their projections on subspaces related to w , such as $(x, w), (x, y, w)$, etc., as the transformed phase portraits (TPP), which may exhibit the relationships between the state variables and the slow variable w .

4.2 Bursting oscillations with codimension-1 bifurcation

For the parameters fixed at $\kappa = 0.5, \delta = -0.15, b = -2.0$ and $c = 0$, which implies that nonlinear terms only up to third order are considered in the function $f(x)$, there are only codimension-1 bifurcations, i.e., fold bifurcations, occurring at the points $FB_{\pm}(x, w) = (\pm\sqrt{6}/6, \pm 2\sqrt{6}/15)$. The bifurcation points divide the x -axis into three parts. When $|x| > \sqrt{6}/6$, only one stable focus exists, while for $|x| < \sqrt{6}/6$, two stable foci as well as a unstable saddle point can be observed. At the bifurcation points $x = \pm\sqrt{6}/6$, one of the two stable foci may meet the saddle point to form a degenerate cusp point, which may lead to the jumping phenomena between different equilibrium points.

While for $\kappa = 0.5, \delta = 0.15, b = -2.0$ and $c = \frac{4}{3}$, implying nonlinear terms up to fifth order are included in the function $f(x)$, there still exist only codimension-1 bifurcations, occurring at the four points $FB_{\pm 1}(x, w) = (\pm 0.470, \pm 0.352)$, $FB_{\pm 2}(x, w) = (\pm 0.824, \pm 0.254)$, leading to the variation of the number of equilibrium points between one, three and five. At the bifurcation points, one stable

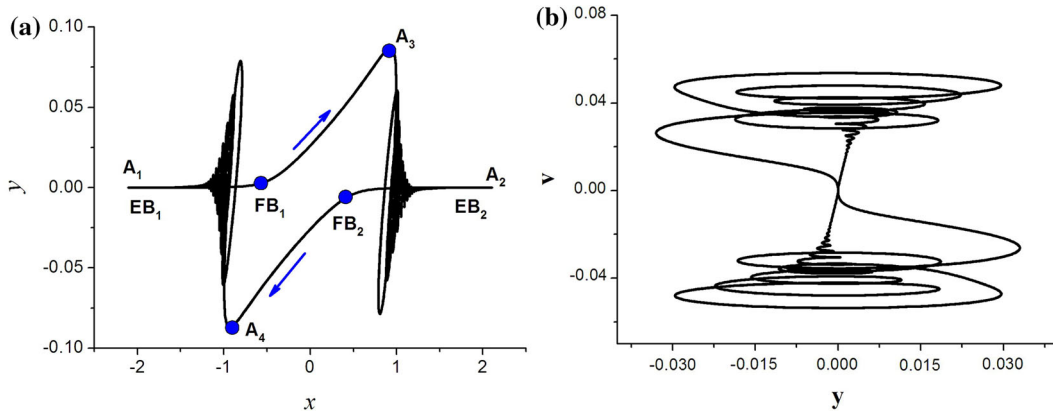


Fig. 3 Phase portraits for $\kappa = 0.5, \delta = -0.15, b = -2.0, c = 0, A = 20.0$ **a** on the (x, y) plane **b** on the (y, v) plane

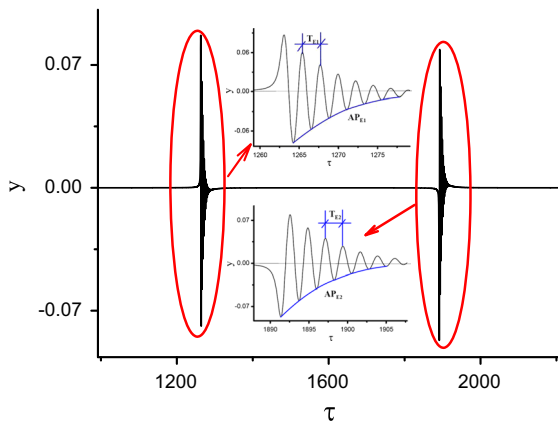


Fig. 4 Time history of y for $\kappa = 0.5, \delta = -0.15, b = -2.0, c = 0, A = 20.0$

focus may meet one unstable saddle point to form a degenerate cusp point, causing the jumping phenomena between different stable equilibrium points.

4.2.1 Bursting oscillations with third-order nonlinear term

Figure 3 gives the phase portrait of the bursting oscillations for $\kappa = 0.5, \delta = -0.15, b = -2.0, c = 0, A = 20.0$, which implies that nonlinear terms only up to third order are considered in the function $f(x)$, and the related time history of y is plotted in Fig. 4.

The trajectory, starting from the point A_1 , moves almost strictly along the stable equilibrium branch EB_1 to form the first stage of quiescent state (QS_1), until it arrives at the bifurcation point FB_1 . Jumping phenomenon occurs, which causes the trajectory to quickly

jump to the point A_3 . Then the trajectory may tend to another equilibrium branch EB_2 , resulting in repetitive spiking (SP_1) with large-amplitude oscillations, since the point A_3 is not exactly located on EB_2 . The amplitudes of the oscillations may gradually decrease, and finally the trajectory may settle down to stable EB_2 to form QS_2 . At the point A_2 , the external excitation reaches its maximum $w = A = 20.0$, which implies w may decrease with the evolution of time. Therefore, the trajectory may return almost strictly along EB_2 until it arrives at the second fold bifurcation point FB_2 . The jumping phenomenon between different equilibrium branches results in the repetitive spiking (SP_2) with large-amplitude oscillations. When the oscillations settle down to the equilibrium branch EB_1 to the point A_1 , one period of the bursting oscillations is finished.

The amplitudes as well as the frequency of the repetitive spiking oscillations can be approximated by the eigenvalues of equilibrium points located on the equilibrium branches. Here we take SP_2 as an example. The spiking oscillations SP_2 may take place between two points on x -axis, denoted by Π_1 and Π_2 , with Π_1 for $x = 0.932$ and Π_2 for $x = 1.491$. The related eigenvalues can be approximated at

$$\begin{aligned} \lambda_1 &= -0.570, & \lambda_2 &= -0.059, & \lambda_{\pm} &= -0.147 \pm 2.740 I, \\ \lambda_1 &= -15.08, & \lambda_2 &= -0.0591, & \lambda_{\pm} &= -0.334 \pm 2.863 I, \end{aligned} \tag{11}$$

at Π_1 and Π_2 , respectively. Therefore, the frequency related to the spiking oscillations may vary from $\Omega_{\Pi_1} \approx 2.740$ to $\Omega_{\Pi_2} \approx 2.863$, which agrees well with the numerical results via $\Omega_{NF} = \frac{2\pi}{T_E}$ varying from 2.764 to 2.881, obtained from the time history in Fig. 3.

The mean frequency of spiking oscillations can be computed at $\Omega_M = \frac{1}{2}(\Omega_{\Pi_1} + \Omega_{\Pi_2}) = 2.802$, yielding the mean period at $T_M = \frac{2\pi}{\Omega_M} \approx 2.242$, while the mean value for the real parts of the pair of the conjugate eigenvalues between Π_1 and Π_2 can be approximated at $Re_M \approx -0.2405$ and the y -value of the SP_2 oscillations may be approximated at $y = Y_A e^{-0.2405(\tau - \tau_0)} \cos[\Omega_M(\tau - \tau_0)]$, where Y_A is the y -value at the beginning of the repetitive spiking with non-dimensional time τ_0 , approximated at $Y_A = -0.0858$ and $\tau_0 = 1891.376$.

The curve $y = Y_A e^{-0.2405(\tau - \tau_0)}$, corresponding to AP_{E2} in Fig. 4, can be used to approximate the amplitudes of the repetitive spiking oscillations, which agrees well with the extreme values of SP_2 . Therefore, the amplitudes of SP_2 oscillations can be approximated at $A_i = |Y_A| e^{-0.5392i}$, ($i = 1, 2, \dots$). For examples, A_2 and A_3 can be theoretically approximated at $A_2 = 0.051$ and $A_3 = 0.010$, respectively, which agrees well with the values of next two amplitudes of spiking oscillations in SP_2 via the numerical simulations (see Fig. 4).

To reveal the mechanism of the bursting oscillations, we plotted the overlap of the transformed phase portrait and the equilibrium branch on the $(x, w) = [x(\tau), A \sin(\Omega\tau)]$ plane in Fig. 5.

The trajectory, starting from the point A_1 , moves almost strictly along the stable equilibrium branch EB_1 to form QS_1 until it arrives at the point FB_1 , at which fold bifurcation occurs, leading to the jumping phenomenon of the trajectory, which may try to approach another stable equilibrium branch EB_2 , yielding repetitive spiking oscillations (SP_1), since the stable EB_1 is stopped at the point B_2 with $(w, x) = (0.3266, -0.4082)$, while EB_3 is unstable branch associated with saddle point. The trajectory in spiking state (SP_2) may tend to the stable equilibrium branch EB_2 via the gradual decrease of the amplitudes of the oscillations, which may finally settle down to EB_2 , leading the second stage of the quiescent state (QS_2). When the trajectory moves at the point A_2 , the external excitation reaches its maximum with $w = A = 20.0$, which may cause the return of the trajectory with further increase of the non-dimensional time τ . The trajectory moves almost strictly along EB_2 , until another fold bifurcation occurs at the point A_3 , which leads to the jumping phenomenon from EB_2 to EB_1 , yielding repetitive spiking oscillations (SP_2). The spiking oscillations may settle down to stable EB_1 , until it reaches the starting point

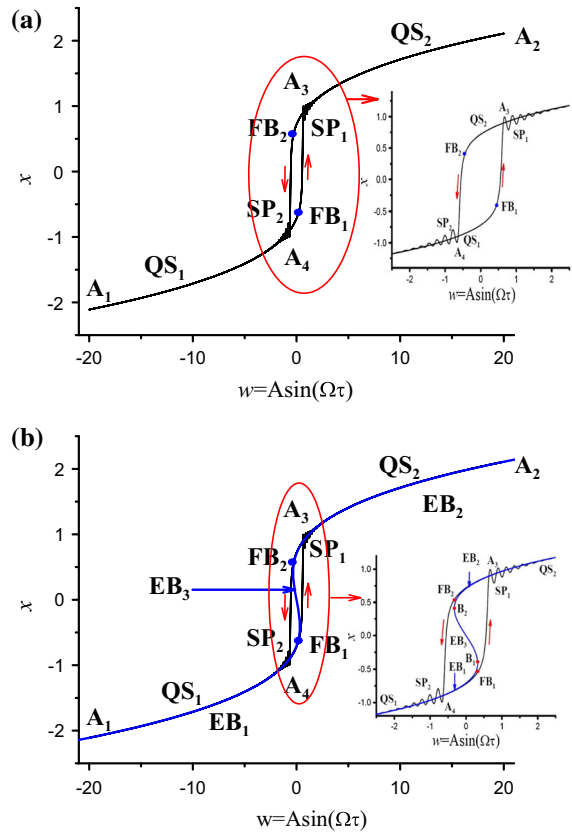


Fig. 5 a Transformed phase portrait b Overlap of the TPP and equilibrium branches of the generalized autonomous system

A_1 , which finishes one period of the bursting oscillations.

Remark 2 \odot There exists very small distance between the fold bifurcation points of the equilibrium branch and connecting points between Qs and SPs on the trajectory, which may be caused by inertia of the trajectory.

\odot The repetitive spiking oscillations are caused by the transient procedures of the trajectory to settle down to the stable equilibrium branches of the generalized autonomous system, in which the fold bifurcation points can be considered as the initial points to approach the focus-type stable equilibrium branches.

4.2.2 Bursting oscillations with fifth-order nonlinear term

Figure 6 gives the phase portrait of the bursting oscillations for $\kappa = 0.5, \delta = 0.15, b = -2.0, c = \frac{4}{3}$ and

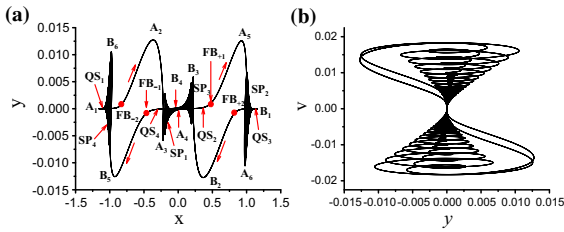


Fig. 6 Phase portraits for $\kappa = 0.5$, $\delta = 0.15$, $b = -2.0$, $c = \frac{4}{3}$ and $A = 1.0$ **a** on the (x, y) plane **b** on the (y, v) plane

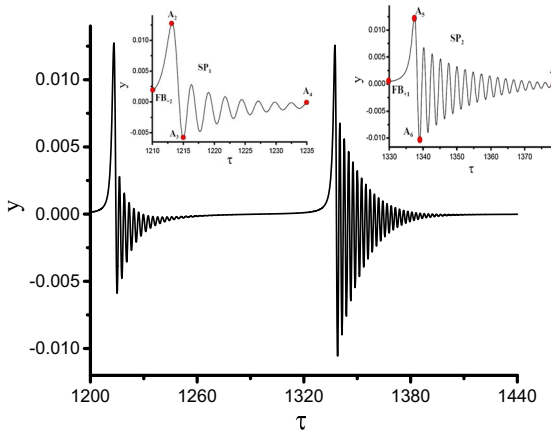


Fig. 7 Time history of y for $\kappa = 0.5$, $\delta = 0.15$, $b = -2.0$, $c = \frac{4}{3}$ and $A = 1.0$

$A = 1.0$, which implies that nonlinear terms up to fifth order are considered in the function $f(x)$, and the related time history of y is plotted in Fig. 7, where only the parts related to SP_1 and SP_2 are presented because of the symmetric structures for SP_3 and SP_4 .

The trajectory, starting from the point A_1 , moves along the curve A_1FB_{-2} , which is almost a straight line with very small y -value, to form QS_1 . When it moves to the point FB_{-2} , fold bifurcation occurs, leading to jumping phenomenon, which results in repetitive spiking oscillations (SP_1). The trajectory quickly passes across the point A_2 to A_3 and oscillates to settle down to the curve A_4FB_{+1} , which is almost a straight line with very small y -value. The trajectory moves along A_4FB_{+1} to form QS_2 until it arrives at the point FB_{+1} , at which another fold bifurcation takes place. Jumping phenomenon appears, leading to the repetitive spiking oscillations SP_2 , which causes the trajectory to quickly pass across A_5 to A_6 and then oscillates around the curve $FB_{+2}B_1$, an almost straight line with very small y -value. When the amplitudes of the oscillations settle

down to zero, the trajectory moves along with the curve $FB_{+2}B_1$ to form QS_3 . The trajectory returns at the point B_1 since the state variable x reaches its maximum and moves along $FB_{+2}B_1$. Fold bifurcation occurs at the point FB_{+2} , leading to the repetitive spiking oscillations SP_3 . The trajectory quickly passes across B_2 to B_3 and oscillates to settle down to the curve B_4FB_{-1} . When the amplitudes of the oscillations decrease to zero, it may move along the curve B_4FB_{-1} , which is an almost straight line with very small y -value, to form QS_4 . Fold bifurcation takes place at the point FB_{-1} , causing the trajectory to quickly pass across B_5 to B_6 . The jumping phenomenon leads to the repetitive spiking SP_4 around the curve A_1FB_{-2} . The gradual decreasing of the amplitudes of the oscillations may lead to the trajectory to settle down to the curve. When the trajectory returns to the point A_1 , one period of the bursting oscillations is finished.

The amplitudes as well as the frequency of the repetitive spiking oscillations can be approximated by the eigenvalues of equilibrium points located on the curves associated, which are almost straight lines with very small y -values by employing the same method for the analysis of the spiking oscillations in Fig. 3. Here we only list the results related to frequencies of the spiking oscillations. For the SP_1 , the spiking oscillations may take place from the point FB_{-2} to A_4 , in which the x -value may vary from -0.824 to -0.0242 , causing the pair of complex conjugate eigenvalues to vary from $-0.4429 \pm 2.050 \text{ I}$ to $-0.0830 \pm 2.289 \text{ I}$. Therefore, the frequency related to SP_1 may increase gradually from 2.050 to 2.289, which agrees very well with the numerical simulations varying from $\frac{2\pi}{2.983} \approx 2.106$ to $\frac{2\pi}{2.741} \approx 2.292$ (see Fig. 7).

Remark 3 Two factors cause the difference between the two frequencies obtained via theoretical method and numerical simulations, respectively. Firstly, the starting point to compute the frequency from time history is taken at A_2 , which is away from the bifurcation point FB_{-2} . Secondly, the absolute value of x for the ending point for numerical computation is taken a bit larger than the absolute value of x at the point A_4 .

To reveal the mechanism of the bursting oscillations, we plotted the overlap of the transformed phase portrait and the equilibrium branches of the generalized autonomous system on the $(x, w) = (x(\tau), A \sin(\Omega\tau))$ plane in Fig. 8.

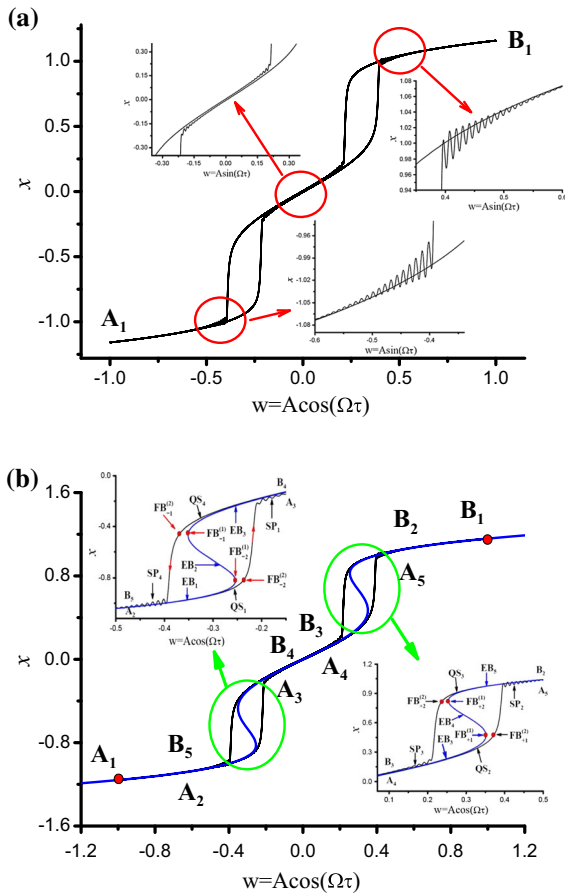


Fig. 8 a Transformed phase portrait on (w, x) b Overlap of the phase portrait and the equilibrium branches

The trajectory, starting from the point A_1 , moves almost strictly along the stable equilibrium branch EB_1 to form QS_1 until it arrives at the point $FB_{-2}^{(2)}$, at which fold bifurcation occurs, leading to the jumping phenomenon of the trajectory, which may try to approach another stable equilibrium branch EB_3 , yielding repetitive spiking oscillations (SP_1). The trajectory in spiking state SP_1 may tend to the stable equilibrium branch EB_3 via the gradual decrease of the amplitudes of the oscillations, and finally settles down to EB_3 , leading the second stage of the quiescent state (QS_2). Trajectory then moves almost strictly along EB_3 until it reaches the point $FB_{+1}^{(2)}$, at which another fold bifurcation takes place. The trajectory may jump to another stable equilibrium branch EB_5 , yielding repetitive spiking oscillations (SP_2), which oscillate around EB_5 . When the trajectory oscillates to settle down to EB_5 , it moves almost strictly along the stable equilibrium

branch EB_5 to form QS_3 . The trajectory may return along EB_5 when it arrives at the point B_1 , at which w reaches its maximum value $w = +1$. The system keeps in quiescent state QS_3 , until the trajectory arrives at the point $FB_{+2}^{(2)}$, at which fold bifurcation occurs, leading to jumping phenomenon of the trajectory to approach EB_3 . Repetitive spiking oscillations SP_3 occur, where the trajectory oscillates around EB_3 . The amplitudes of the oscillations may gradually decrease and finally settle down to zero. Then the trajectory moves almost strictly along EB_3 to form QS_4 until the trajectory arrives at the point $FB_{-1}^{(2)}$, at which fold bifurcation occurs. Jumping phenomenon can be observed, which may cause the trajectory to oscillate around the stable equilibrium branch EB_1 via repetitive spiking oscillations (SP_4). The amplitudes of the oscillations may gradually settle down to zero, causing the trajectory to move almost strictly along the stable EB_1 . When the trajectory arrives at the starting point A_1 , one period of the movement is finished.

Remark 4 \odot From the overlap of the transformed phase portrait and the equilibrium branches in Fig. 8b, one may find that there exists a bit difference between the theoretical fold bifurcation points and the corresponding connecting points between Qs and SPs on the trajectory, which may be caused by the inertia of the trajectory since the nominal parameter w is not static, but changes slowly with the non-dimensional time τ .

\odot The spiking oscillations are caused by the transient procedures of the trajectory to approach the stable focus-type equilibrium branches, since the trajectory at the fold bifurcation points may jump from one equilibrium branch to another focus-type equilibrium branch. Therefore, the fold bifurcation points, located near the corresponding bifurcation points on one equilibrium branch, can be considered as the initial points to approach another equilibrium branch. Because of the focus-type of the equilibrium branch, the trajectory may cycle around the equilibrium branch to settle down to the branch, which may cause the spiking oscillations around the corresponding equilibrium branch.

4.3 Bursting oscillations with codimension-2 bifurcation

When the conditions in (8) are satisfied, codimension-2 bifurcation (fold-Hopf bifurcation) associated with

a zero and a pair of pure imaginary eigenvalues may take place. For the parameters fixed in (9) and $\kappa = 1.0, \delta = -0.15, b = -2.0, c = 0$, which implies that nonlinear terms only up to third order are considered in the function $f(x)$, there exist codimension-2 bifurcations, i.e., the combination of fold and Hopf bifurcations, occurring at the points $FB_{\pm}(x, w) = (\pm\frac{\sqrt{6}}{6}, \pm\frac{2\sqrt{6}}{15})$. While for $\kappa = 1.0, \delta = 0.15, b = -2.0, c = \frac{4}{3}$, implying that nonlinear terms up to fifth order are included in the function $f(x)$, codimension-2 bifurcations may occur at the four points $FB_{\pm 1}(x, w) = (\pm 0.470, \pm 0.352), FB_{\pm 2}(x, w) = (\pm 0.824, \pm 0.254)$. The codimension-2 bifurcations may cause different structures of bursting attractors, since there exist not only the jumping phenomena between different equilibrium branches, but also limit cycle oscillations with the frequency $\sqrt{\beta}$. In the following, we will investigate the bursting oscillations as well as the mechanism for the two cases with different orders of nonlinear terms in the function $f(x)$.

4.3.1 Bursting oscillations with third-order nonlinear terms

Figure 9 gives the phase portrait of the bursting oscillations for $\kappa = 1.0, \delta = -0.15, b = -2.0, c = 0$ and $A = 20.0$, which implies that nonlinear terms only up to third order are considered in the function $f(x)$, and the related time history of y is plotted in Fig. 10, where only one period is presented.

The phase portrait of the bursting oscillations with codimension-2 bifurcations connecting the quiescent states (QSs) and spiking states (SPs) is greatly different from that of the bursting attractors with codimension-1 bifurcations between QSs and SPs. The trajectory may oscillate around two cycles, which may be caused

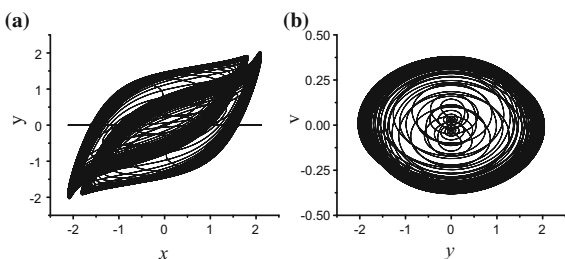


Fig. 9 Phase portraits for $\kappa = 1.0, \delta = -0.15, b = -2.0, c = 0$ and $A = 20.0$ a on the (x, y) plane b on the (y, v) plane

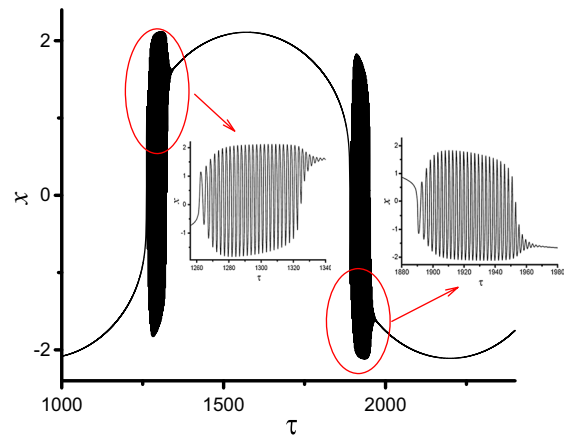


Fig. 10 Time history of x for one period

by the super-Hopf bifurcation part included in the codimension-2 bifurcations (see Fig. 8a), while the fold bifurcation part included in the codimension-2 bifurcation may lead to the jumping phenomenon between the two oscillations around the two cycles (see Fig. 9b), which can also be demonstrated by the time history of x plotted in Fig. 10.

It can be found that the structures of two SPs are symmetric to each other because of the symmetry of the system. When spiking oscillations occur from a QS, which is almost strictly located on one equilibrium branch via a codimension-2 bifurcation, the trajectory does not try to settle down to another equilibrium branch, but to oscillate to an large-amplitude cycle with the increase of the amplitudes of the oscillations. Therefore, the codimension-2 bifurcation causes not only the jumping phenomenon, but also limit cycle oscillations. When the amplitudes of the oscillations increase to an extent, the trajectory may oscillate to settle down to another QS with gradual decrease of the amplitudes of the oscillations.

To reveal the mechanism of the bursting oscillations, we plot the related transformed phase portrait in Fig. 11. The trajectory, starting from the point A_1 , moves along $A_1A_2A_3$ to form QS_1 . A codimension-2 bifurcation causes the trajectory to jump to the repetitive spiking oscillations (SP_1). The amplitudes of the oscillations increase with the evolution of the non-dimensional time τ until the trajectory reaches the potential limit cycle. Then the amplitudes of the oscillations may decrease to settle down to QS_2 . Similar situations occur when the trajectory returns from the maximum value of w at B_1 .

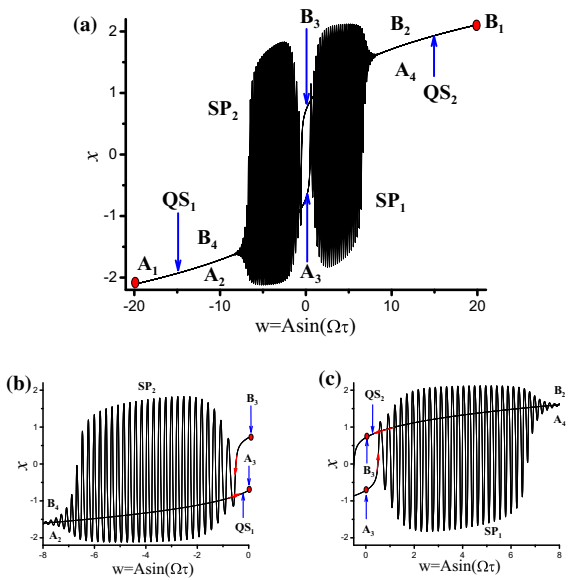


Fig. 11 a Transformed phase portrait b and c Locally enlarged TPP

More clear mechanism for the bursting oscillations can be observed in Fig. 12, in which the overlap of the transformed phase portrait and the equilibrium branches is plotted. The trajectory, starting from the point A_1 , moves almost strictly along EB_1 to form QS_1 until it reaches the point $B_{-1}^{(1)}$, at which a codimension-2 bifurcation occurs, not only leading to the jumping phenomenon to the equilibrium branch EB_3 , but also causing the trajectory to approach the limit cycle via repetitive spiking (SP_1). The amplitude of the limit cycle, caused by super-Hopf bifurcation part included in the codimension-2 bifurcation, may increase with the increase of w , which leads to the increase of amplitudes of the spiking oscillations. Further increase of w may cause the gradual decrease of the amplitude of the oscillations, because of the attraction of the stable focus-type equilibrium branch EB_3 . The trajectory may gradually settle down to EB_3 to form QS_2 and returns when w reaches its maximum value at $w = 20.0$. Then the trajectory moves almost strictly along the equilibrium branch EB_3 , until it arrives at another codimension-2 bifurcation point $B_{+1}^{(1)}$. The bifurcation not only causes the jumping phenomenon from EB_3 to EB_1 , but also leads to the repetitive spiking oscillations around potential limit cycle to form SP_2 . When the trajectory settles down to EB_1 and moves to the starting point A_1 , one period of the bursting oscillations is finished.

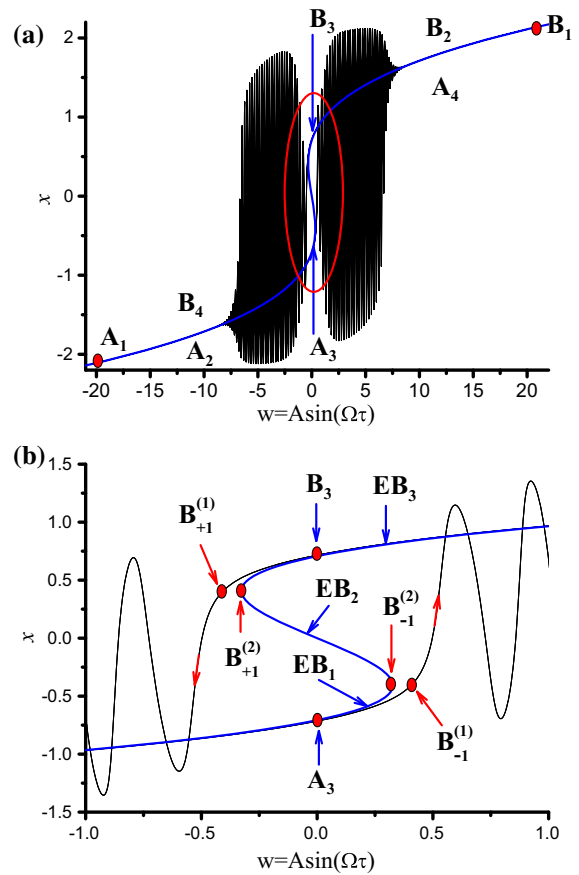


Fig. 12 a Overlap of the transformed phase portrait and the equilibrium branches b Locally enlarged of the overlap

4.3.2 Bursting oscillations with fifth-order nonlinear terms

When nonlinear terms up to fifth order are included in the function, another two codimension-2 bifurcation points can be observed on the equilibrium branches of the generalized autonomous system. Figure 13 gives the overlap of the transformed phase portrait and the equilibrium branches for the bursting oscillations with $\kappa = 1.0, \delta = 0.15, b = -2.0, c = \frac{4}{3}$ and $A = 10.0$, while the phase portrait as well as the time history is a bit similar to those of the bursting oscillations in Figs. 8 and 9.

The trajectory, starting from the point A_1 in Fig. 13a, moves almost strictly along the equilibrium branch EB_1 to form QS_1 , until it arrives at the point $B_{-2}^{(1)}$, which is very close to the point $B_{-2}^{(2)}$ on EB_1 , at which a codimension-2 bifurcation occurs, causing the tra-

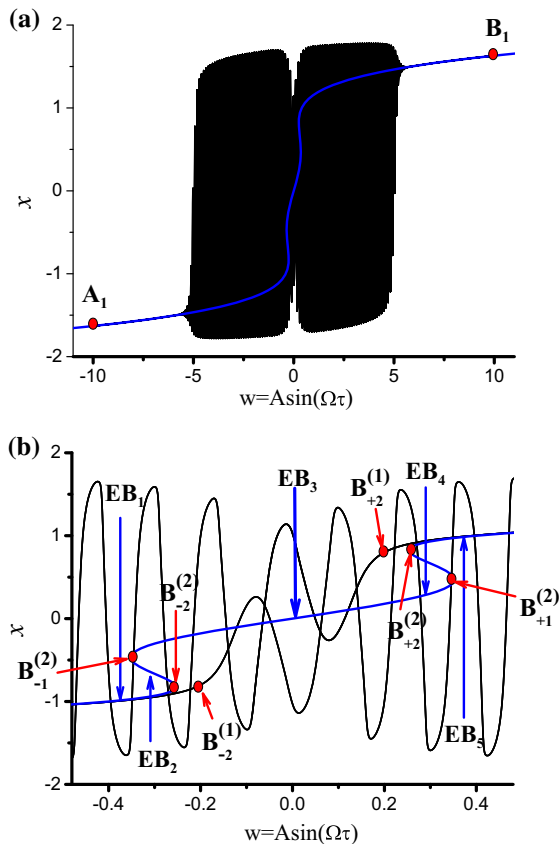


Fig. 13 **a** Overlap of the transformed phase portrait and the equilibrium branches for the bursting oscillations with fifth order nonlinear term **b** Locally enlarged of the overlap

jectory to jump to the stable focus-type equilibrium branch EB_3 . Note that the x -value of the point on EB_3 is between the two codimension-2 bifurcation points $B_{-1}^{(2)}$ and $B_{+1}^{(2)}$, and the trajectory may oscillate to the potential cycle around EB_3 , starting the stage of SP_1 . When the trajectory moves near the bifurcation point $B_{+1}^{(2)}$, it turns to oscillate to the potential limit cycle around EB_5 . When the amplitudes of the oscillations reach the maximum value, they may gradually decrease to settle down to EB to start the second stage of quiescent state QS_2 . Then the trajectory moves almost strictly along EB_5 to the point B_1 , at which w reaches its maximum value. The trajectory may return along EB_5 . Similar phenomenon can be observed for pross for trajectory to return to the starting point A_1 .

Since two different limit cycles around EB_3 may appear from the codimension-2 bifurcation points $B_{-2}^{(1)}$ and $B_{+2}^{(1)}$, respectively, the trajectory cannot settle down

to EB_3 . Similarly, two limit cycles around EB_1 and EB_5 , respectively, may bifurcate from $B_{-1}^{(1)}$ and $B_{+1}^{(1)}$, which may lead to the alternation between the oscillations around EB_1 and EB_3 or between the oscillations around EB_3 and EB_5 .

5 Conclusions

When an order gap exists between the periodically exciting frequency and the natural frequency, bursting oscillations alternating between quiescent states (Qs) and repetitive spiking states (SPs) may be observed. For the case when exciting frequency is far smaller than the natural frequency, the whole exciting term can be regarded as a small-varying parameter, leading to a so-called generalized autonomous system, which can be considered as a fast subsystem. The equilibrium states as well as the related bifurcations of the fast subsystem determine the forms of Qs and SPs as well as the bifurcations between Qs and SPs. Therefore, when higher-order nonlinear terms are included in the vector fields, more equilibrium points as well as the related bifurcations may involve the structure of the bursting attractors, which may lead to more complicated bursting oscillations. Furthermore, bifurcations with high codimension may result in complicated transitions between Qs and SPs, which may also cause the complexity of the bursting attractors.

References

1. Abobda, L.T., Wofo, P.: Subharmonic and bursting oscillations of a ferromagnetic mass fixed on a spring and subjected to an AC electromagnet. *Commun. Nonlinear Sci. Numer. Simul.* **17**, 3082–3091 (2012)
2. Courbage, M., Maslennikov, O.V., Nekorkin, V.I.: Synchronization in time-discrete model of two electrically coupled spike-bursting neurons. *Chaos Solitons Fractals* **45**, 645–659 (2012)
3. Tsaneva-Atanasova, K., Osinga, H.M., Rieß, T., Sherman, A.: Full system bifurcation analysis of endocrine bursting models. *J.Theor. Biol.* **264**, 1133–1146 (2010)
4. Shilnikov, A.: Complete dynamical analysis of a neuron model. *Nonlinear Dyn.* **68**, 305–328 (2012)
5. Simo, H., Wofo, P.: Bursting oscillations in electromechanical systems. *Mech. Res. Commun.* **38**, 537–541 (2011)
6. Kingni, S.T., Keuninckx, L., Wofo, P., Sande, G., Danckaert, J.: Dissipative chaos, Shilnikov chaos and bursting oscillations in a three-dimensional autonomous system: theory and electronic implementation. *Nonlinear Dyn.* **73**, 1111–1123 (2013)

7. Watts, M., Tabak, J., Zimlik, C., Sherman, A., Bertram, R.: Slow variable dominance and phase resetting in phantom bursting. *J. Theor. Biol.* **276**, 218–228 (2011)
8. Izhikevich, E.: Neural excitability, spiking and bursting. *Int. J. Bifurc. Chaos* **10**, 1171–1266 (2000)
9. Schaffer, W.M., Bronnikova, V.: Peroxidase-ROS interactions. *Nonlinear Dyn.* **68**, 413–430 (2012)
10. Shen, J.H., Zhou, Z.Y.: Fast–slow dynamics in first-order initial value problems with slowly varying parameters and application to a harvested logistic model. *Commun. Nonlinear Sci. Numer. Simul.* **19**, 2624–2631 (2014)
11. Wang, X.Y., Wang, L., Wu, Y.J.: Novel results for a class of singular perturbed slow–fast system. *Appl. Math. Comput.* **225**, 795–806 (2013)
12. Rush, M.E., Rinzel, J.: The potassium a-current, low firing rates and rebound excitation in Hodgkin–Huxley models. *Bull. Math. Biol.* **57**, 899–929 (1995)
13. Li, Y.X., Rinzel, J.: Equations for InsP₃ receptor-mediated [Ca²⁺] Oscillations derived from a detailed kinetic model: a Hodgkin–Huxley like formalism. *J. Theor. Biol.* **166**, 461–473 (1994)
14. Izhikevich, E.M., Desai, N.S., Walcott, E.C., Hoppensteadt, F.C.: Bursts as a unit of neural information: selective communication via resonance. *Trends Neurosci.* **26**, 161–167 (2003)
15. Kingni, S.T., Nana, B., Ngueuteu, G.S.M., Wofo, P., Danckaert, J.: Bursting oscillations in a 3D system with asymmetrically distributed equilibria: mechanism, electronic implementation and fractional derivation effect. *Chaos Solitons Fractals* **71**, 29–40 (2015)
16. Medetov, B., Weiß, R.G., Zhanabaev, ZZ, Zaks, M.A.: Numerically induced bursting in a set of coupled neuronal oscillators. *Comm. Nonlinear Sci. Numer. Simul.* **20**, 1090–1098 (2015)
17. Yu, Y., Tang, H.J., Han, X.J., Bi, Q.S.: Bursting mechanism in a time-delayed oscillator with slowly varying external forcing. *Commun. Nonlinear Sci. Numer. Simul.* **19**, 1175–1184 (2014)
18. Han, X.J., Jiang, B., Bi, Q.S.: Symmetric bursting of focus–focus type in the controlled Lorenz system with two time scales. *Phys. Lett. A* **373**, 3643–3649 (2009)
19. Bi, Q.S., Zhang, Z.D.: Bursting phenomena as well as the bifurcation mechanism in controlled Lorenz oscillator with two time scales. *Phys. Lett. A* **375**, 1183–1190 (2011)
20. Wierschem, K., Bertram, R.: Complex bursting in pancreatic islets: a potential glycolytic mechanism. *J. Theor. Biol.* **228**, 513–521 (2004)
21. Han, X.J., Bi, Q.S.: Bursting oscillations in Duffings equation with slowly changing external forcing. *Commun. Nonlinear Sci. Numer. Simul.* **16**, 4146–4152 (2011)
22. Zheng, S., Han, X.J., Bi, Q.S.: Bifurcations and fast-slow behaviors in a hyperchaotic dynamical system. *Commun. Nonlinear Sci. Numer. Simul.* **16**, 1998–2005 (2011)
23. Rasmussen, A., Wyller, J., Vik, J.O.: Relaxation oscillations in spruce–budworm interactions. *Nonlinear Anal. Real World Appl.* **12**, 304–319 (2011)
24. Perc, M., Marhl, M.: Different types of bursting calcium oscillations in non-excitable cells. *Chaos Solitons Fractals* **18**, 759–773 (2003)
25. Zhang, Z.D., Li, Y.Y., Bi, Q.S.: Routes to bursting in a periodically driven oscillator. *Phys. Lett. A* **377**, 975–980 (2013)
26. Skeldon, A.C., Moroz, I.M.: On a codimension-three bifurcation arising in a simple dynamo model. *Phys. D* **117**, 117–127 (1998)
27. DaCunha, J.J., Davis, J.M.: A unified Floquet theory for discrete, continuous, and hybrid periodic linear systems. *J. Differ. Equ.* **251**, 2987–3027 (2011)
28. Munyon, C., Eakin, K.C., Sweet, J.A., Miller, J.P.: Decreased bursting and novel object-specific cell firing in the hippocampus after mild traumatic brain injury. *Brain Res.* **1582**, 220–226 (2014)
29. Masaud, K., Macnab, C.J.B.: Preventing bursting in adaptive control using an introspective neural network algorithm. *Neurocomputing* **136**, 300–314 (2014)
30. Barnett, W., O’Brien, G., Cymbalyuk, G.: Bistability of silence and seizure-like bursting. *J. Neurosci. Methods* **220**, 179–189 (2013)
31. Simo, H., Wofo, P.: Bursting oscillations in electromechanical systems. *Mech. Res. Commun.* **38**, 537–541 (2011)
32. Jothimurugan, R., Suresh, K., Ezhilarasu, P.M., Thamilmaran, K.: Improved realization of canonical Chua’s circuit with synthetic inductor using current feedback operational amplifiers. *AEU Int. J. Electron. Commun.* **68**, 413–421 (2014)
33. Zou, Y.L., Zhu, J.: Controlling the chaotic n-scroll Chua circuit with two low pass filters. *Chaos Solitons Fractals* **29**, 400–406 (2006)
34. Dai, H.H., Yue, X.K., Xie, D., Atluri, S.N.: Chaos and chaotic transients in an aeroelastic system. *J. Sound Vib.* **333**, 7267–7285 (2014)
35. Ghosh, D., Chowdhury, A.Y., Saha, P.: Bifurcation continuation, chaos and chaos control in nonlinear Bloch system. *Commun. Nonlinear Sci. Numer. Simul.* **13**, 1461–1471 (2008)